# Stability of the High-Latitude Reconnection Site for Steady Northward IMF

S. A. Fuselier, S. M. Petrinec, K. J. Trattner

*Lockheed Martin Advanced Technology Center, Palo Alto, CA*

**Abstract:** The stability of the high-latitude reconnection site under steady northward Interplanetary Magnetic Field (IMF) conditions was investigated using observations in the Earth's magnetospheric cusp. Using proton distributions with characteristic low-energy cutoffs, the distance from the spacecraft to the high-latitude reconnection site was monitored during four cusp crossings that had relatively steady solar wind dynamic pressure and IMF clock angle. For these four events, the reconnection site location remained approximately fixed, indicating that the high-latitude magnetic reconnection site remains stable for many minutes under steady IMF conditions. A possible explanation for this stability is that the magnetosheath flow remains sub-Alfvenic even at high latitudes because of the presence of a plasma depletion layer.

## Introduction

Magnetic reconnection is an important process for the transfer of mass, energy, and momentum from the Earth's magnetosheath across the magnetopause and into the magnetosphere. The effectiveness of this transfer process depends on the rate of reconnection and the location of reconnection on the magnetopause. It is therefore critical to determine how these reconnection characteristics depend on external conditions in the solar wind.

Observations of temporal variations of the precipitating magnetosheath ion energy in the magnetospheric cusps have been used as evidence that the rate of reconnection is almost never steady [e.g., Lockwood and Smith, 1992]. These same cusp observations can be interpreted in

terms of variations in other parameters such as the location of the reconnection site [e.g., Fuselier et al., 1999], or changes in other conditions at the magnetopause [e.g., Trattner et al., 1999]. Although there are several possible interpretations, these cusp observations appear to provide a good indication of variations in reconnection parameters at the magnetopause.

There have been few studies of the stability of the magnetopause reconnection site location (i.e., the stability of the neutral line location). In situ observations of ion and electron distributions in the magnetopause reconnection layers yield a direction to the reconnection site [e.g., Paschmann et al., 1986] and, in special cases, yield a distance to the reconnection site [e.g., Onsager and Fuselier, 1994]. However, it is difficult to investigate long term changes in the location of this site because spacecraft reside in these layers for at most a few minutes during a magnetopause crossing. Nonetheless, there are reports of changes in the reconnection site location over periods of several minutes [e.g., Gosling et al., 1991].

The above evidence of changes in reconnection parameters suggests that this process may never occur stably over long periods of time in a fixed location on the magnetopause. Computer simulations may support this suggestion. Although they do not address the reconnection rate, simulations of the global interaction of the solar wind with a model magnetosphere indicate that the location of reconnection can change even for relatively steady solar wind conditions. Global MHD simulations of magnetopause reconnection at high latitudes for northward IMF suggest that the reconnection site may shift tailward by 12 $R_E$ over a 30 min interval starting 10 min after the IMF rotated from southward to northward [Berchem et al., 1995]. Although the change from southward to northward IMF may have an important influence in these simulations, large-scale hybrid simulations suggest otherwise. In these hybrid simulations, the reconnection site forms at the high-latitude magnetopause for steady northward IMF and then convects rapidly tailward (on the time scale of minutes), reforming later near its initial location [Omidi et al., 1998].

There is good reason to suspect that the high latitude reconnection site may not remain in a fixed location. If reconnection is initiated at high latitudes tailward of the point where the

magnetosheath flow becomes super-Alfvenic, then the reconnection site may have to move tailward such that the sheath flow is Alfvenic in the rest frame of the site [e.g., Gosling et al., 1991].

In this paper, the stability of the reconnection site for northward IMF, steady solar wind conditions is investigated using observations in the cusp. These observations are from the Polar spacecraft, which is in a 90˚ inclination orbit that periodically passes through the cusp at high altitudes (4-6 $R_E$).

## Reconnection for Northward IMF

When the IMF is northward, magnetic reconnection may occur on lobe field lines poleward of the magnetospheric cusps (see, however alternate reconnection locations in Fuselier et al., [1999]). Observations of sunward convection of reconnected field lines and the velocity dispersion of precipitating magnetosheath ions associated with this convection are evidence of the high-latitude reconnection site [e.g., Matsuoka et al., 1996]. The ions are dispersed such that the highest energy ions precipitate furthest poleward and successively lower energy ions precipitate equatorward of this high-latitude boundary. High altitude spacecraft (e.g., the Polar spacecraft) observe both the precipitating magnetosheath ions propagating parallel to the magnetic field (in the northern cusp) and magnetosheath ions propagating antiparallel to the magnetic field that have convected to their mirror points in the ionosphere and returned to the spacecraft.

It is well known from observations in the Earth's plasma sheet boundary layer that the precipitating and mirrored ion populations can be used to estimate the distance to the reconnection site [e.g., Onsager et al., 1991]. Ions near the low-energy cutoffs of the precipitating and mirrored populations come from near the reconnection site. By equating the travel times of the ions at these two cutoffs, the ratio of the distance from the spacecraft to the reconnection site ($X_r$) to the distance from the spacecraft to the mirror point ($X_m$) is:

$$X_r / X_m = 2 V_e / (V_m - V_e) \quad (1)$$

Here, $V_e$ is the cutoff speed of the precipitating (earthward propagating) population and $V_m$ is the cutoff speed of the mirrored population. For the observations presented below, the spacecraft position and the Tsyganenko 1996 (T96) model were used to determine $X_m$ and $V_e$ and $V_m$ were determined from low-speed cutoffs in proton distributions in the cusp.

**Observations in the Cusp**

Figure 1 shows the spacecraft location for a cusp event on 7 May 1996. The noon-midnight meridonal cut through the T96 model is shown. During the cusp event, the solar wind dynamic pressure (derived from the solar wind plasma measurements from the Wind spacecraft located 45 $R_E$ upstream from the Earth) was nearly constant at 2.4 nPa, (i.e., near its nominal value of ~1.5 nPa). Furthermore, the IMF clock angle ($\arctan(B_y/B_z)$, from the magnetometer measurements on Wind) was nearly due northward (-13˚) and varied by about ±4˚ during the cusp crossing. Thus, during the cusp crossing in Figure 1, the spacecraft was on field lines poleward of the cusp (i.e. field lines that map to the nightside magnetotail) and the solar wind pressure and IMF direction were nearly constant.

As is common of cusp observations for northward IMF, the Toroidal Imaging Mass-Angle Spectrograph (TIMAS) on the Polar spacecraft [Shelley et al., 1995] observed precipitating magnetosheath ions whose mean energy increased with increasing latitude. This energy-latitude dispersion is consistent with magnetic reconnection at high latitudes poleward of the cusp and sunward convection of the reconnected magnetic field lines. Figure 2 contains representative proton observations from the cusp crossing in Figure 1 that illustrate the energy-latitude dispersion. Shown are cuts parallel to the magnetic field through three proton pitch angle distributions (all in the spacecraft frame of reference) observed at three different latitudes. The

solid line shows the log of the phase space density and the dashed line shows the 1-σ level. Cut A represents the proton observations at the highest cusp latitudes. The cut shows a downward (toward the ionosphere) propagating magnetosheath proton population with a peak velocity of about 350 km/s.

Cut B represents observations at lower cusp latitudes and shows three proton populations. The first is a downward propagating (toward the ionosphere) magnetosheath population with a peak velocity of about 175 km/s and a distinct "low-speed cutoff" of about 100 km/s. The second population is cold and propagating upward (from the direction of the ionosphere) with a peak velocity of about -25 km/s. The cold temperature, low velocity, and direction of propagation of this population are all consistent with an ionospheric proton population. Ionospheric outflow of this type is commonly seen at these latitudes [e.g., Yau et al., 1985]. The third population is propagating upward with a peak velocity of -500 km/s and a distinct low-speed cutoff of -475 km/s. The phase space density, direction of propagation, and low-speed cutoff of this population are all consistent with magnetosheath protons that have propagated along the field, mirrored at low altitudes, and returned to the spacecraft.

Cut C in Figure 2 appears to be a single proton population with a peak velocity of 75-100 km/s. However, peaks in the proton population at positive and negative velocities suggest the presence of three proton populations similar to those in cut B.

The low-speed cutoffs in cut B in Figure 2 are used in (1) to determine the distance to the reconnection site. Since the TIMAS instrument obtains a full 3-D proton distribution every 12 s, the distance to the reconnection site can be determined at this rate, so long as distinct proton populations as in cut B are observed. In this study, the low-speed cutoff is defined as the point (at lower absolute velocity) where the phase space density of a population is 1/e of the peak phase space density. The uncertainty in the low-speed cutoff is defined as 1/2 the difference between the peak speed and the low-speed cutoff. The low-speed cutoffs and their uncertainties are shown in cuts A and B in Figure 2. Cut A does not have a mirrored magnetosheath population antiparallel

to the magnetic field (above the 1-σ level). For this cut, any mirrored population must be at velocities less than ~-800 km/s since the source of these ions is the population propagating parallel to the magnetic field. Thus, while the distance to the reconnection site cannot be determined from this cut, the maximum distance can be determined by using the low-speed cutoff of the downgoing population and by setting $V_m$ = 800 km/s in (1). Cut C shows evidence of downgoing and upgoing populations. However, the low-speed cutoffs for the parallel propagating population is probably quite small and the mirrored population has apparently merged with the ionospheric population. Since no low-speed cutoffs can be measured for cut C, the distance to the reconnection site cannot be determined.

From cuts similar to A and B in Figure 2, the distance to the reconnection site ($X_r$) could be monitored nearly continuously at 12 s resolution for about 20 min during the crossing in Figure 1. The top panel in Figure 3 shows the $X_r$ profile during this time interval. Solid circles show $X_r$ determined from cuts similar to B in Figure 2. Open circles show the maximum distance to the reconnection site determined from cuts similar to A in Figure 2. The shaded region below the open circles implies that the reconnection site may be located at any distance from zero to the maximum distance. For the period from 0515 to 0517, cuts similar to C in Figure 2 were obtained and $X_r$ could not be determined.

The uncertainties in $X_r$ in Figure 3 vary dramatically and are due entirely to the uncertainties in $V_m$ and $V_e$. For example, the uncertainty in $X_r$ is fairly small (~±1 $R_E$) for cut B in Figure 2, because the low-speed cutoffs are reasonably well defined. However, the uncertainty in $X_r$ is larger (~±2 $R_E$) for cut A in Figure 2 because $V_e$ is less well defined. The weighted mean of $X_r$ (i.e., the mean when each measurement is weighted by its uncertainty) is 3.8 $R_E$ (the horizontal line in the top panel of Figure 3). This average distance and a range of ±2 $R_E$ about this average distance (representing an approximate range of $X_r$) is shown in Figure 1 to illustrate how much the reconnection site location may change compared to the scalesize of the magnetosphere.

The next 3 panels in Figure 3 show the distances to the reconnection site computed from observations made during 3 other cusp events similar to the one in Figure 1. In all cases the solar wind dynamic pressure was 2-2.5 nPa and the IMF clock angle was steady. The IMF clock angles were different for each of the events in Figure 4. For 7 May 1996, the clock angle was -13˚, for 23 May it was 60-80˚, for 28 May it was 55˚, and for 6 Nov., it was 30-50˚.

## Discussion

Although the cusp events in Figure 4 had significantly different IMF clock angles, they all show a more or less steady distance to the reconnection site for ~15 to 20 min intervals. This is long compared to the convection time of a parcel of magnetosheath plasma near the high-latitude magnetopause. The magnetosheath bulk flow velocity near the +Z terminator must be a significant fraction of the solar wind velocity and a parcel of plasma at this point will move at least 30-40 $R_E$ during a typical 15-20 min monitoring of the reconnection site location. There is no evidence of significant (>10 $R_E$) movement of the reconnection site in Figure 4 as suggested by computer simulations discussed in the introduction [Berchem et al., 1995; Omidi et al., 1998]. Concerning this issue, the IMF profile during the 23 May event was similar to that used in the MHD simulation discussed in the introduction. It was southward at 0630-0640 UT (~10-20 min prior to the first determination of the distance to the reconnection site). For ~10 min after the northward turning (from 0650-0700 UT), the distance to the reconnection site could be determined. Then there was a 25 min period from 0705 - 0730 UT when cuts similar to C in Figure 2 were obtained and no distance could be determined. After this 25 min interval, the distance to the reconnection site was found to be at the same distance or even closer to the spacecraft than the distance determined soon after the northward turning of the IMF. In contrast, the reconnection site moved tailward by ~12 $R_E$ during a 30 min interval after the northward turning of the IMF in the MHD simulation discussed in the introduction [Berchem et al., 1995].

There may be evidence for smaller changes in $X_r$, such as the change from ~3 to 7 $R_E$ from 0524 to 0526 UT on 7 May or from ~6 to 10 $R_E$ from 1301 to 1302 UT on 6 November. However, with $X_r$ uncertainties of ~1-2 $R_E$, one could also argue that the distance did not change at all or changed very little during these time periods.

Given the stability of the reconnection site location for long periods of time, it is important to consider why high-latitude reconnection sites in fast magnetosheath bulk flows could remain in a fixed location. The acuteness of the problem is illustrated in Figure 4. The short curves identified by dates are the average location of the reconnection site (±2 $R_E$) for the 4 events in Figure 3 rotated into the X, Z GSM plane. For the average dynamic pressure of ~2.5 nPa, the magnetopause has a subsolar standoff distance just inside 10 $R_E$. The ratio of the bulk flow speed to the Alfven speed ($V_{msh}/V_{Alfven}$) along the magnetopause was computed from polynomial fits to the gas-dynamic results of Spreiter and Stahara [1985] for the magnetosheath density, bulk velocity, and magnetic field [see Onsager et al., 1995]. These ratios are shown at several locations along the magnetopause starting at $X_{GSM}$ = 9 $R_E$ and extending past the terminator. The ratio becomes greater than one at $X_{GSM}$ <8.5 $R_E$. Three of the four reconnection site locations were well into the super-Alfvenic regime of the magnetosheath flow. A similar result was inferred from lower latitude observations of sunward flows in the cusp [Matsuoka et al., 1996]. Although Matsuoka et al. did not determine the distance to the reconnection site, they were able to infer that the reconnection site was located at high latitudes where the flow should be super-Alfvenic.

In super-Alfvenic flow, a reconnection site must move tailward so that the bulk flow speed in the frame of reference where the electric fields vanish on both side of the discontinuity (i.e., the deHoffman-Teller frame) is Alfvenic. The tailward speed of the reconnection site would increase as the bulk flow along the magnetopause increases. Matsuoka et al. [1996] suggested a rather complex explanation for the reason why apparent sunward convection of the reconnected field line could be observed even when the reconnection site moved tailward. However, the observations in

Figure 3 show that the high-latitude reconnection site does not move tailward, in disagreement with their explanation.

There may be a simple explanation for a fixed high-latitude reconnection site. The Spreiter and Stahara [1985] model does not include the magnetic field in a self-consistent manner. Therefore, it does not include the effects of the formation of a plasma depletion layer along the magnetopause. This depletion layer causes the magnetic field to increase by about a factor of 2 over the nominal magnetosheath value and the plasma density to decrease by a similar amount over its nominal magnetosheath value. At the subsolar point, this would imply an Alfven speed of ~2.8 times higher than that predicted from the Spreiter and Stahara model. Allowing the same variation in the magnetic field, plasma density, and bulk flow velocity along the magnetopause as in the Spreiter and Stahara model but starting with the higher magnetic field and lower density in the subsolar depletion layer, a second set of $V_{msh}/V_{Alfven}$ values are listed in parentheses along the magnetopause in Figure 4. Including the effects of a depletion layer in this simple manner keeps the flow sub-Alfvenic up to and past the terminator. This may provide a simple and readily testable explanation for the stability of the high-latitude reconnection site location. There has already been at least one report of approximately Alfven flow at the magnetopause near the high-latitude terminator [Gosling et al., 1991].

**Acknowledgments:** We thank T. Onsager for useful discussions. The IMF and Solar Wind Plasma data were obtained from the CDAWeb. The authors thank R. Lepping and K. Ogilvie for providing these data and C. Russell for providing the Polar Magnetometer data. The TIMAS instrument is the result of many years of work by a dedicated group of scientists and engineers.

**References**

Berchem, J., J. Raeder, and M. Ashour-Abdalla, Reconnection at the magnetospheric boundary: Results from global magnetohydrodynamic simulations, in *Physics of the Magnetopause, Geophys. Monogr. Ser. vol. 84,* edited by P. Song, B. U. Ö Sonnerup, and M. F. Thomsen, p. 205, AGU, Washington, D. C., 1995.

Fuselier, S. A., K. J. Trattner, and S. M. Petrinec, Cusp observations of high- and low-latitude reconnection for northward IMF, J. Geophys. Res., in press, 1999.

Gosling, J. T., M. F. Thomsen, S. J. Bame, R. C. Elphic, and C. T. Russell, Observations of reconnection of interplanetary and lobe magnetic field lines at the high-latitude magnetopause, *J. Geophys. Res., 96,* 14,097, 1991.

Matsuoka, A., K. Tsuuruda, H. Hayakawa, T. Mukai, and A. Nishida, Electric field structure and ion precipitation in the polar region associated with northward interplanetary magnetic field, *J. Geophys. Res., 101,* 10,711, 1996.

Omidi, N., P. Riley, H. Karimabadi, and D. Krauss-Varban, Global hybrid simulations of solar wind-magnetosphere interactions: Scalability of the results, *EOS Trans. Amer. Geophys. U., 79, no. 45,* F749, 1998.

Onsager, T. G., M. F. Thomsen, R. C. Elphic, and J. T. Gosling, Model of electron and ion distributions in the plasma sheet boundary layer, *J. Geophys. Res., 96,* 20,999, 1991.

Onsager, T. G., and S. A. Fuselier, The location of magnetic reconnection for northward and southward interplanetary magnetic field, in *Solar System Plasmas in Space and Time, Geophys. Monogr. Ser. vol. 84,* edited by J. L. Burch and J. H. Waite, Jr., p. 183, AGU, Washington, D. C., 1994.

Onsager, T. G., S.-W. Chang, J. D. Perez, J. B. Austin, and L. X. Janou, Low-altitude observations and modeling of quasi-steady magnetopause reconnection, *J. Geophys. Res., 100,* 11,831, 1995.

Paschmann, G., I. Papamastorakis, W. Baumjohann, N. Sckopke, C. W. Carlson, B. U. Ö. Sonnerup, and H. Lühr, The magnetopause for large magnetic shear: AMPTE/IRM observations, *J. Geophys. Res., 91,* 11,099, 1986.

Shelley, E. G., et al., The toroidal imaging mass-angle spectrograph (TIMAS) for the Polar mission, in *The Global Geospace Mission,* ed. by C. T. Russell, p. 497, Kluwer Academic Publishers, Dordrecht, 1995.

Spreiter J. R., and S. S. Stahara, Magnetohydrodynamic and gasdynamic theories for planetary bow waves, in Collisionless Shocks in the Heliosphere: Reviews of Current Research, Geophys. Monogr. Ser., vol. 35, edited by B. T. Tsurutani and R. G. Stone, p. 85, AGU, Washington, D. C., 1985.

Trattner, K. J., S. A. Fuselier, W. K. Peterson, J.-A. Sauvaud, H. Stenuit, N. Dubouloz, and R. A. Kovrazhkin, On spatial and temporal structures in the cusp, *J. Geophys. Res.*, in press, 1999.

Yau, A. W., E. G. Shelley, W. K. Peterson, and L. Lenchyshyn, Energetic auroral and polar ion outflow at DE 1 altitudes: Magnituce, cmpoosition, magnetic activity dependence, and long-term variations, *J. Geophys. Res., 90,* 8417, 1985

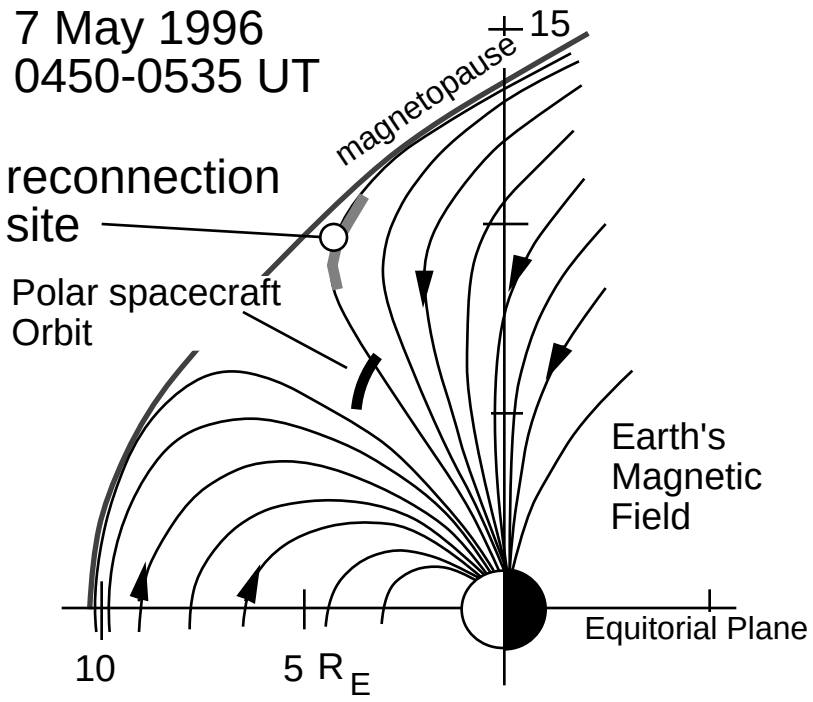


Figure 1. T96 magnetosphere model showing the location of the Polar spacecraft and the average location of the reconnection site on 7 May 1996 from 0518-0534 UT.

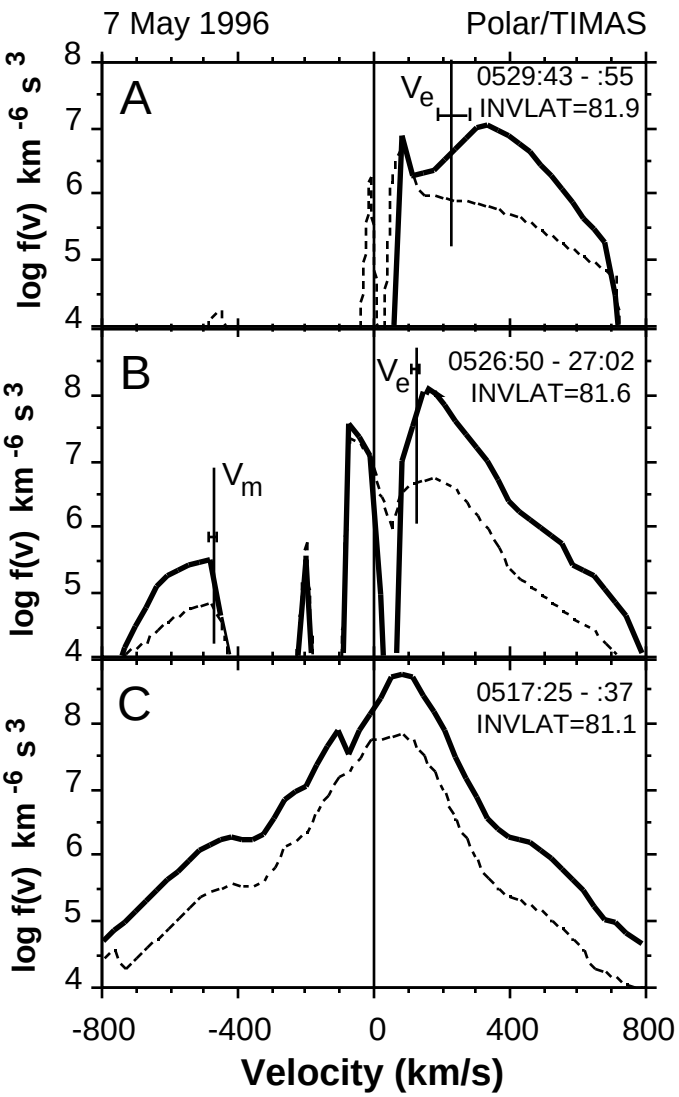


Figure 2. Cuts parallel to the magnetic field through three proton distributions observed on 7 May 1996. Cut A contains a downgoing magnetosheath proton population. Cut B contains downgoing and upcoming magnetosheath proton populations as well as a cold, upcoming ionospheric population at low velocity. Cut C may contain the same populations as cut B but the distinction between them is difficult.

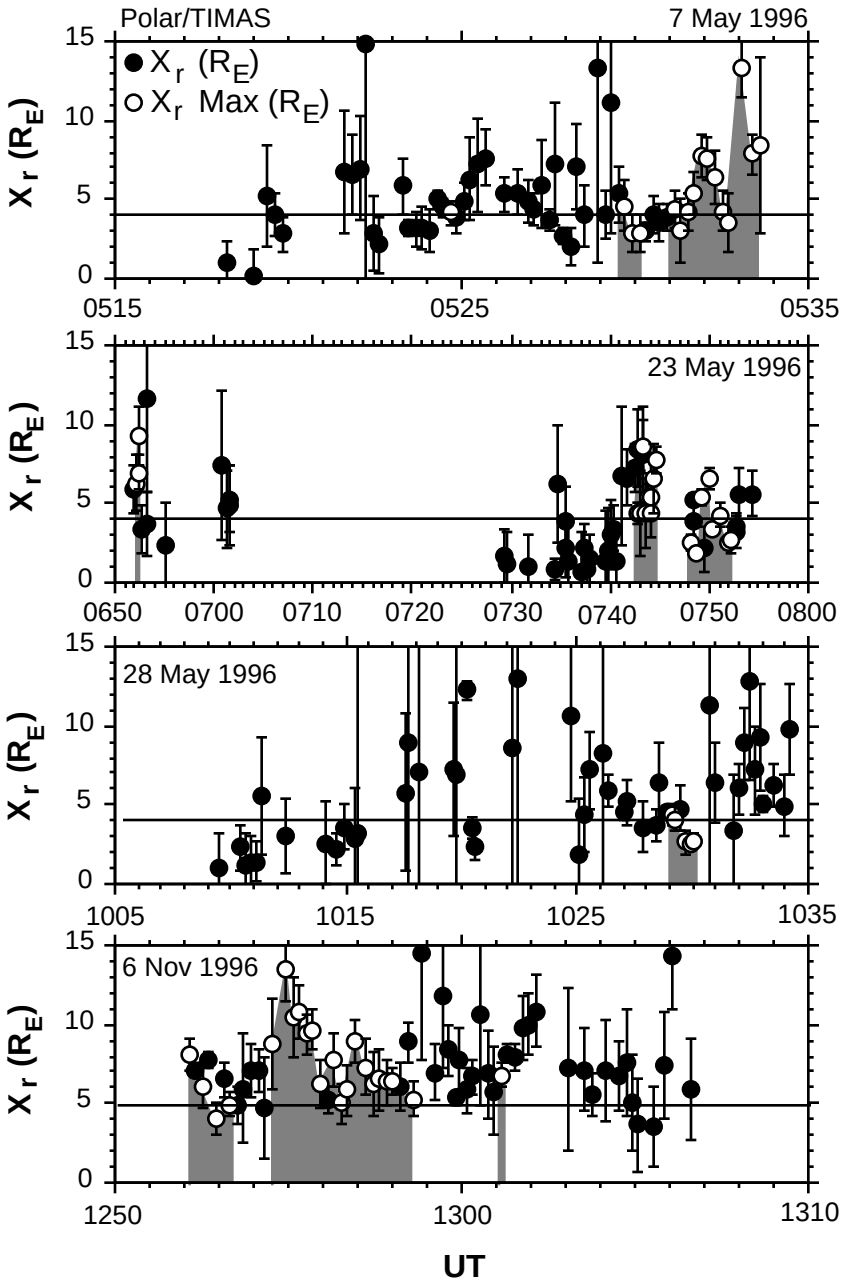


Figure 3. Distance from the spacecraft to the reconnection site for 4 cusp crossings. The distance remains relatively constant during each event.

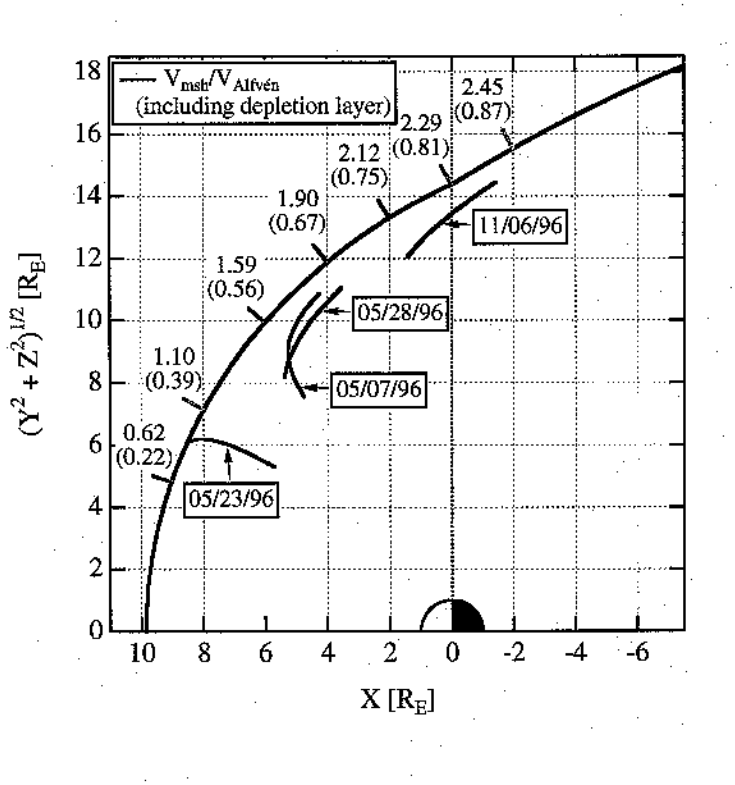


Figure 4. $V_A/V_{sheath}$ versus distance along the magnetopause (from the Spreiter and Stahara gasdynamic model). Three of four reconnection sites are well within super-alfvenic flow unless the presence of a depletion layer is taken into account.